Journal of Environmental Economics and Management 109 (2021) 102462

Contents lists available at ScienceDirect

Journal of Environmental Economics and Management

journal homepage: www.elsevier.com/locate/jeem

Global vulnerability of crop yields to climate change☆,☆☆,☆☆☆

Ian Sue Wing [a,*], Enrica De Cian [b], Malcolm N. Mistry [b]

[a] Dept. of Earth & Environment, Boston University, USA
[b] University Ca' Foscari of Venice and Centro Euro-Mediterraneo sui Cambiamenti Climatici (CMCC), Italy

ARTICLE INFO

JEL classification:
N5
O13
Q1
Q54

Keywords:
Panel data
Climate change
Adaptation
Crop yields

ABSTRACT

Using a newly-available panel dataset of gridded annual crop yields in conjunction with a dynamic econometric model that distinguishes between farmers' short-run and long-run responses to weather shocks and accounts for adaptation, we investigate the risk to global crop yields from climate warming. Over broad spatial domains we observe only slight moderation of short-run impacts by farmers' long-run adjustments. In the absence of additional margins of adaptation beyond those pursued historically, projections constructed using an ensemble of 21 climate model simulations suggest that the climate change could reduce global crop yields by 3–12% by mid-century and 11–25% by century's end, under a vigorous warming scenario.

1. Introduction

There has long been concern about the potential risks to crop production posed by projected shifts in the Earth's climate, and the extent to which agricultural systems will be able to adapt to these changes to sustain food supplies. While recent research has sought to address this question by elucidating how farmers have historically been able to adapt to temperature and precipitation shifts (Blanc and Reilly, 2017), the issue is far from settled. Meta-analyses suggest that adaptation could prevent most yield losses for wheat and rice (Challinor et al., 2014), and cross-sectional studies of the response of land values or farm revenue to different locations to variations in climate caution that estimates of the negative effects of climate change that omit adaptation are likely overstated (Mendelsohn and Massetti, 2017). By contrast, the bulk of the empirical climate change economics literature uses cross-section/time-series econometric modeling to estimate the responses of crop yields to weather shocks, which addresses the potential for adaptation only implicitly (Dell et al., 2014). A key exception is Burke and Emerick (2016), who employ a long-differences approach to highlight that adjustments of maize and soybean cultivation in the United States (US) over time-frames of decades or more have resulted in only modest attenuation of the adverse effects of extreme heat exposures on yield losses. Burke and Emerick show that if such limits to adaptation persist, projected increases in growing season temperatures due to climate change portend substantial yield declines. These findings raise the possibility that the challenge of adapting to climate warming may be pervasive. The fact that US lies at the world technological frontier

☆ Ian Sue Wing was supported by the U.S. Department of Energy, Office of Science, Biological and Environmental Research Program, Earth and Environmental Systems Modeling, MultiSector Dynamics, Contract No. DE-SC0016162.
☆☆ Enrica De Cian gratefully acknowledges support from the People Programme Marie Curie Actions of the European Union (FP7/2007–2013) REA grant agreement No. 298436 and from CMCC.
☆☆☆ Malcolm N. Mistry gratefully acknowledges support from Ca' Foscari University of Venice.
* Corresponding author. Dept. of Earth & Environment, Boston University, 675 Commonwealth Ave., Boston, MA, 02215, USA.
E-mail addresses: isw@bu.edu (I.S. Wing), enrica.decian@unive.it (E. De Cian), malcolm.mistry@unive.it (M.N. Mistry).

https://doi.org/10.1016/j.jeem.2021.102462
Received 20 August 2019; Received in revised form 31 March 2021; Accepted 21 April 2021
Available online 27 May 2021

bodes ominously for future yields and production in technologically less advanced agricultural systems, particularly in the tropics where 40% of the world's population live and extreme high temperature increases are projected to exceed those in the US. Moreover, the fact that maize and soybeans account for nearly half of the world's supply of dietary energy suggests that resulting risks to world food supplies could be severe—even in the presence of farmers' adjustments.

In this paper we investigate the impacts of climate change on crop yields across the globe in the presence of agricultural adaptation, focusing on maize, rice, wheat and soybeans, which together account for 75% of global dietary energy intake (Cassman, 1999). Using a newly-available panel dataset of gridded annual crop yields, we statistically distinguish between farmers' responses to weather shocks in the short run and the long run in different agroclimatic zones across the globe. We infer adaptation as the difference between long-run and short-run yield responses to weather in a dynamic empirical model, an approach that differs from Burke and Emerick's comparison between static panel and long difference responses.[1]

Our long-run semi-elasticities of yield to temperature and precipitation exposure are consistent with Burke and Emerick's findings, and, critically, show that they generalize to additional crops as well as to agricultural systems across the world. We assess the consequences for climate change impacts on crop yields in different locations by combining these estimates with changes in exposure to different intervals of temperature and precipitation at the middle and the end of the century calculated from an ensemble of simulations of 21 earth system models (ESMs). As early as mid-century, under vigorous warming most crops experience declining yields across more than 75% of the places where they are cultivated, with distributions of yield shocks that in the long run show only slightly attenuation—and in a few cases amplification—relative to those in the short run. The variance of the distributions of yield shocks arises predominantly out of variation in temperature and precipitation exposures across locations as opposed to among ESM simulations, which across crops substantially agree on yield reductions in response to vigorous warming of $<$10% circa 2050 and $<$25% circa 2090.

The rest of the paper is organized as follows. Section 2 presents and discusses our dynamic empirical model of yield responses to weather in the short- and the long-run. Section 3 describes the data used, and the econometric issues that arise in operationalizing this model. Section 4 describes the empirical results, with a detailed discussion of regional vulnerabilities to the adverse effects of weather extremes and the role of irrigation in moderating them. Section 5 uses the estimated semi-elasticities to temperature and precipitation exposure to calculate climate-induced changes in crop yields under future climate. Section 6 concludes with a brief summary of our findings, major caveats, and potential directions for future research.

2. Empirical approach: a dynamic model of agricultural production and yield adjustment

Our empirical model of yields is derived from crop producers' maximization of expected profit. Adapting the static production framework of Pope and Just (1996) and Moschini (2001), a representative price-taking farmer's profit function is denominated over yield (Y) and vectors of input prices (deflated by the price of output, $\mathbf{W}$), uncertain weather exposures ($\mathcal{E}$), and exogenous factors ($\mathbf{X}$): $\Pi(Y,\mathbf{W},\mathcal{E},\mathbf{X})$. When actual weather exposures align with expectations (indicated using a star), ex-post profit is in equilibrium with its ex-ante target level: $\Pi^{\star}(Y^{\star},\mathbf{W},\mathcal{E}^{\star},\mathbf{X})$. Static profit maximization describes farmers' within-growing-season behavior for field crops that follow regular planting and harvesting cycles. We assume that from one crop cycle to the next the producer determines the adjustment of profit to its equilibrium level within a dynamic adjustment cost framework (Nickell, 1985; Hallam and Zanoli, 1993; Fanelli, 2006). Conditional on the information available at each time period (t), the farmer minimizes expected discounted adjustment costs made up of two components: the divergence of profit from its target equilibrium level and the inter-period variance of profit. We show in Appendix A that the solution to this problem is a partial adjustment process for profit, which, when the profit function takes a loglinear form, implies the follow error correcting process for yield:

$$\Delta y_t = \alpha + \gamma + \boldsymbol{\beta}' \Delta \mathcal{E}_t + \boldsymbol{\delta}' \Delta \mathbf{x}_t - \Omega[y_{t-1} - \boldsymbol{\eta}' \mathcal{E}_{t-1} - \boldsymbol{\xi}' \mathbf{x}_{t-1} - \gamma t] + v_t \tag{1}$$

in which Δ indicates inter-period differences, and y and $\mathbf{x}$ denote the logarithms of yield and other observables.

For the purposes of empirical analysis we model each location in our dataset (which we index using i) as a representative producer. In this setup, the trending levels and constant average rates of growth of prices, technology and (perhaps to a lesser extent) profit expectations are likely be similar for multiple grid cells. Given the likelihood of different locations within the same country sharing institutional and economic fundamentals, we assume that α is a grid-cell level fixed effect capturing unobserved heterogeneous location-specific time-invariant influences, while γ varies over countries, $j(i)$. We further allow the profit function to vary geographically, particularly in response to weather exposures, which influence yield expectations and farmers' static and dynamic calculus. We therefore group grid cells into agroclimatic zones or irrigation regimes, $z(i)$, and stratify the parameters $\boldsymbol{\beta}$, $\boldsymbol{\delta}$, $\boldsymbol{\eta}$ and $\boldsymbol{\xi}$ and Ω accordingly. Expressing weather exposures as vectors of growing season days associated with different intervals of temperature ($\mathcal{E}^T$) and precipitation ($\mathcal{E}^P$), we arrive at our final panel error-correction model (ECM) specification:

$$\begin{aligned}\Delta y_{i,t} = \quad & \alpha_i + \gamma_{j(i)} + \sum_{z(i)} \left\{ \boldsymbol{\beta}_z^{T'} \Delta \mathcal{E}_{i,t}^{T} + \boldsymbol{\beta}_z^{P'} \Delta \mathcal{E}_{i,t}^{P} + \boldsymbol{\delta}_z' \Delta \mathbf{x}_{i,t} \right\} \\ & - \sum_{z(i)} \Omega_z \left[y_{i,t-1} - \boldsymbol{\eta}_z^{T'} \mathcal{E}_{i,t-1}^{T} - \boldsymbol{\eta}_z^{P'} \mathcal{E}_{i,t-1}^{P} - \boldsymbol{\xi}_z' \mathbf{x}_{i,t-1} - \gamma_{j(i)} t \right] + u_{i,t}\end{aligned} \tag{2}$$

[1] We also use Burke and Emerick (2016) adaptation metric for comparison and robustness checks. See Section 4.

This specification decomposes observed yield adjustments into short- and long-run components. The first component is identified by the interannual covariation between yields and meteorology, captured by the first-difference terms in curly braces. We attribute the corresponding parameters, $\boldsymbol{\beta}$, to farmers' responses to weather shocks over the short run, over which no adaptation occurs. The second component is identified by the average covariation between yield changes and past meteorology, captured by the lagged terms in square braces. We attribute the corresponding parameters, $\boldsymbol{\eta}$, to farmers' long-run responses to climate. Given the long time-frame of these adjustments, we assume that they represent farmers' adaptation. It is useful to understand how our ECM specification relates to existing empirical models. Eq. (2) is a representation of the equivalent Autoregressive Distributed Lag (ADL) Model (1,1) model:

$$\begin{aligned} y_{i,t} = \quad & \alpha_i + \sum_{z(i)} \Big\{ \Big(1-\Omega_z\Big) y_{i,t-1} + \gamma_{j(i)}(1+\Omega_z)t + \boldsymbol{\beta}_z^{T'} \mathcal{E}_{i,t}^{T} + \boldsymbol{\beta}_z^{P'} \mathcal{E}_{i,t}^{P} + \boldsymbol{\delta}_z' \mathbf{x}_{i,t} \\ & + \left(\Omega_z \boldsymbol{\eta}_z^{T} - \boldsymbol{\beta}_z^{T}\right)' \mathcal{E}_{i,t-1}^{T} + \left(\Omega_z \boldsymbol{\eta}_z^{T} - \boldsymbol{\beta}_z^{T}\right)' \mathcal{E}_{i,t-1}^{P} + \left(\Omega_z \boldsymbol{\xi}_z - \boldsymbol{\delta}_z\right)' \mathbf{x}_{i,t-1} \Big\} + u_{i,t} \end{aligned} \tag{3}$$

which encompasses two limiting cases: permanent shocks ($\Omega_z \to 0$) which give rise to the first-difference specification with no adjustment:

$$\Delta y_{i,t} = \alpha_i + \gamma_{j(i)} + \sum_{z(i)} \Big(\boldsymbol{\beta}_z^{T'} \Delta \mathcal{E}_{i,t}^{T} + \boldsymbol{\beta}_z^{P'} \Delta \mathcal{E}_{i,t}^{P} + \boldsymbol{\delta}_z' \Delta \mathbf{x}_{i,t} \Big) + u_{i,t}^{\text{First Difference}} \tag{4}$$

and instantaneous adjustment ($\Omega_z \to 1$) which gives rise to the static specification with lagged covariates:

$$\begin{aligned} y_{i,t} = \quad & \alpha_i + 2\gamma_{j(i)}t + \sum_{z(i)} \Big\{ \boldsymbol{\beta}_z^{T'} \mathcal{E}_{i,t}^{T} + \boldsymbol{\beta}_z^{P'} \mathcal{E}_{i,t}^{P} + \boldsymbol{\delta}_z' \mathbf{x}_{i,t} \\ & + \left(\boldsymbol{\eta}_z^{T} - \boldsymbol{\beta}_z^{T}\right)' \mathcal{E}_{i,t-1}^{T} + \left(\boldsymbol{\eta}_z^{T} - \boldsymbol{\beta}_z^{T}\right)' \mathcal{E}_{i,t-1}^{P} + \left(\boldsymbol{\xi}_z - \boldsymbol{\delta}_z\right)' \mathbf{x}_{i,t-1} \Big\} + u_{i,t}^{\text{Static-Lag}} \end{aligned} \tag{5}$$

The latter specification differs from the traditional static model (e.g., Schlenker and Roberts, 2009; Fisher et al., 2012; Blanc and Schlenker, 2017):

$$y_{i,t} = {}^{*}\alpha_i + {}^{*}\gamma_{j(i)}t + \sum_{z} \Big\{ {}^{*}\boldsymbol{\eta}_z^{T'} \mathcal{E}_{i,t}^{T} + {}^{*}\boldsymbol{\eta}_z^{P'} \mathcal{E}_{i,t}^{P} + {}^{*}\boldsymbol{\xi}_z' \mathbf{x}_{i,t} \Big\} + {}^{*}u_{i,t}^{\text{Static}} \tag{6}$$

In particular, (5) and (6) converge to the long-run effect ($\boldsymbol{\eta} = {}^{*}\boldsymbol{\eta}$ and $\boldsymbol{\xi} = {}^{*}\boldsymbol{\xi}$) only in expectation, a fact that we can use to derive Burke and Emerick's long difference estimator. Averaging the dependent and independent variables over n time periods, we define $\overline{y}_{i,t} = \frac{1}{n}\sum_{\tau=-n/2}^{n/2} y_{i,t+\tau}$, $\overline{\mathcal{E}}_{i,t} = \frac{1}{n}\sum_{\tau=n/2}^{n/2} \mathcal{E}_{i,t+\tau}$ and $\overline{\mathbf{x}}_{i,t} = \frac{1}{n}\sum_{\tau=n/2}^{n/2} \mathbf{x}_{i,t+\tau}$. Taking similar averages of (3) for sufficiently large n, the fact that $\overline{y}_{i,t-1} \to \overline{y}_{i,t}$, $\overline{\mathcal{E}}_{i,t-1} \to \overline{\mathcal{E}}_{i,t}$ and $\mathbf{x}_{i,t-1} \to \mathbf{x}_{i,t}$ suggests that differencing the resulting expression for two points in time $> n$ periods apart gives rise to the cross-sectional regression:

$$\Delta \overline{y}_i = \gamma_{j(i)} \Delta t + \sum_{z} \Big\{ \boldsymbol{\eta}_z^{T'} \Delta \overline{\mathcal{E}}_i^{T} + \boldsymbol{\eta}_z^{P'} \Delta \overline{\mathcal{E}}_i^{P} + \boldsymbol{\xi}_z' \Delta \overline{\mathbf{x}}_i \Big\} + u_i^{\text{Long Difference}} \tag{7}$$

whose parameters are identical to our long-run effect. The key implication is that our estimates of long-run responses of yields to temperature and precipitation are directly comparable to Burke and Emerick, with the principal difference between their approach and ours being the "no adaptation" counterfactual to which the long run is compared. Their measure of adaptation is $1 - \boldsymbol{\eta}/{}^{*}\boldsymbol{\eta}$ whereas ours is $1 - \boldsymbol{\eta}/\boldsymbol{\beta}$. If substantial historical adaptation occurred, we would expect to see $\|\boldsymbol{\eta}\| \ll \|\boldsymbol{\beta}\|$.

3. Data and econometric issues

3.1. Data

There are two principal data inputs to our econometric model. For our dependent variable we used an unbalanced panel of annual yields of four major crops (maize, soybean, rice and spring and winter wheat) recorded across the world on a 1.125° grid for the period 1981–2011 (Iizumi et al., 2014; Iizumi and Ramankutty, 2016). The dataset downscales time series of annual production and harvested area at the country level maintained by the U.N. Food & Agriculture Organization (FAO), using gridded data on historical remotely sensed net primary productivity (NPP) from the U.S. National Oceanic and Atmospheric Administration's Advanced Very High Resolution Radiometer (NOAA/AVHRR).[2] Our meteorological covariates were derived from historical 3-hourly global surface temperature and precipitation fields on a 0.25° grid from the Global Land Data Assimilation System (GLDAS) (Rodell et al., 2004),

[2] Given our empirical approach, obvious concerns are that these yield estimates rely on meteorological information for their construction, and yield measurements may be contaminated by accounting for greenness not associated to crop yields. While we have verified that this is not the case through extensive personal communications with the dataset's author, we discuss the potential limitations of employing downscaled crop yields in Section 6. More details of the dataset are provided in the Appendix.

matched to the years above.

Several modifications to these data were necessary to get them into a form suitable for estimation of eq. (2). Fine scale meteorological fields were aggregated to match the coarser spatial resolution of the yield dataset and truncated within each year to a fixed crop- and cell-specific growing season defined by a global crop calendar dataset of planting and harvesting dates circa year 2000 (Sacks et al., 2010). We considered the main cropping season only, which reduced the spatial extent of some crops (e.g., rice in China—see Fig. 1).[3] We then temporally aggregated the resulting array of growing season weather to construct fields of daily mean temperature and total precipitation, which we subsequently binned into counts of daily exposure in 14 temperature intervals and 12 precipitation intervals. These are our exposure covariates, $\mathcal{E}^T$ and $\mathcal{E}^P$.

With respect to crop prices, we use country-level prices from the FAOSTAT database.[4] To use these data would require us to forgo a significant share of our observations, and therefore we always show results with and without prices.

At the global scale of our study, we need to consider the possibility that the manner in which yields respond to weather will vary across the different management regimes and climates in which a given crop is grown. The likely effect is heterogeneity in the estimated parameters of eq. (2). We therefore allow them to vary geographically in two different ways. We first consider variation according to management regime. To operationalize this, we classify grid cells as irrigated or rainfed using the MIRCA2000 dataset of irrigated areas (Portmann et al., 2010), in conjunction with the M3-Cropland dataset of harvested area by crop (Monfreda et al., 2008). As both of these datasets are static, circa year 2000, we have no choice but to apply the same classification to every year in our sample period. For each crop, irrigated grid cells were defined as those for which the crop in question constituted at least 10% of the cell's total harvested area, and the irrigated fraction of the cell exceeded the rainfed fraction.

The second possibility we consider follows from eq. (A.1), namely, that across dissimilar climates, differences in producers' target yields in response to weather expectations generate dynamics of adjustment to weather shocks that vary systematically over space. Exploiting the high spatial resolution of the crop yield data, we apply *k*-means clustering (Hartigan and Wong, 1979) to identify swaths of contiguous grid cells that share similar long-term average values of yields, growing season temperature and precipitation. The number of clusters was not pre-defined, but was determined by the algorithm based on the data. For each crop, three broad groupings were identified, which we attribute to agroclimatic zones.[5]

The two stratifications are mapped in Fig. 1, which the world's major areas of high yields and intensive cultivation of calorie crops—the so-called "calorie sheds" of the US midwest, northeastern China, northern India, and the southeastern portions of Europe and S. America—are clearly visible. Summaries of harvested area, yields and weather exposures for the full slate of calorie crops are given in the Appendix (Table A.1, Fig. A.2). The majority of grid-cells are rainfed. In irrigated cultivation, the largest fraction of harvested area is accounted for by rice (37%), followed by maize (24%), winter wheat (20%), soybeans (12%), and spring wheat (9%). Rice, soybeans, and maize are grown in cells with higher average growing season temperatures (21–24 °C) compared to wheat (7–17 °C). Soybeans and rice cultivation is concentrated in areas with moderate total growing season precipitation, while irrigated maize and winter wheat are grown in dry conditions (mean precipitation of only 13 and 6 mm). Interestingly, only for maize, rice, and winter wheat do cells with rainfed and irrigated production differ substantially in the amount of total precipitation.

Crop yields are consistently higher in irrigated areas. Looking at characteristics of crops grown across the different agroclimatic zones, crops grown under drier climate include maize in zone 3, winter wheat in zone 2 and 3, and spring wheat across all zones. Spring wheat, however, is also grown at average low temperatures. Rice and soybeans in zone 1 and maize in zone 3 are grown also under relatively low precipitation levels, if compared to the other zones with the same crop, or even to irrigated rice and soybeans, which have on average higher precipitation levels. The highest temperature conditions are found in rice zone 2 and 3, soybeans zone 2 and 3, maize zone 1 and 3. Note that maize grown in zone 3 accounts for the 15% of harvested grid cells. Maize in zone 3 has also the highest productivity (1.5 tons/ha in log), a value that is only slightly lower to the productivity of irrigated maize (1.5 tons/ha) and rice (1.4 tons/ha). We expect the most vulnerable crops to be maize in zone 3, rice in zone 1, soybeans and winter wheat in zone 2 and 3.

Our projections of yield impacts are constructed from average weather exposures $\widetilde{\mathcal{E}}_0^T$, $\widetilde{\mathcal{E}}_0^P$, $\widetilde{\mathcal{E}}_{t^*}^T$ and $\widetilde{\mathcal{E}}_{t^*}^P$ derived from the NASA Earth Exchange Global Daily Downscaled Projections (NEX-GDDP) dataset. NEX-GDDP is a large ensemble of downscaled and biased-corrected 0.25° gridded daily meteorological fields from 21 ESMs that simulate vigorous (RCP 8.5) and moderate (RCP 4.5) warming under the Coupled Model Intercomparison, Phase V (CMIP5) climate model exercise. Daily mean temperature and precipitation over the 1986–2005 historical period ($t = 0$), and for the 2041–2060 mid-century and 2080–2099 late-century periods ($t = t^*$), were truncated to the growing seasons of our five crops, binned to generate counts of daily exposure in the same temperature and precipitation intervals as our historical dataset, and stratified geographically according to our irrigation and agroclimatic zones in Fig. 1. The resulting exposure projections were combined with our fitted temperature and precipitation semi-elasticities to calculate the fractional changes in the yields of individual crops (see Section 5).

3.2. Econometric issues

We run separate panel regressions for each crop. Even with our large sample, multicollinearity precluded identification of the

[3] Yield in the main cropping season is highly correlated with FAO reported yields.

[4] FAO data accessed from www.fao.org on January 2020.

[5] Since the agroclimatic zones are identified also on the basis of average yield conditions, they also reflect differences in long-term average technology, land quality, and input availability, see (Ramankutty et al., 2018).

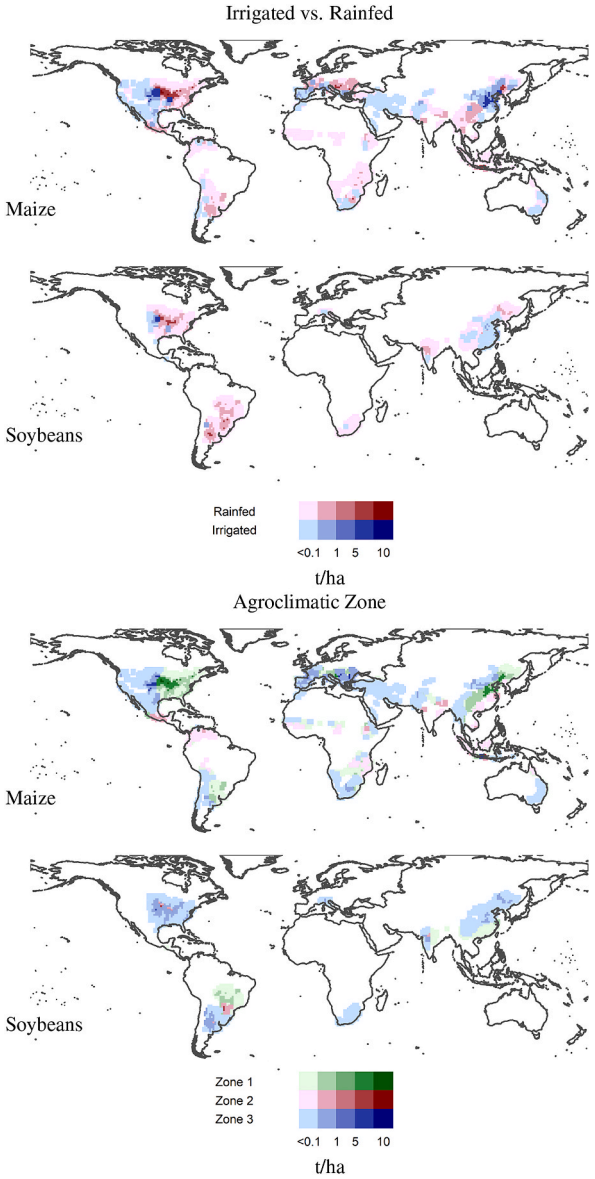

Fig. 1. Geographic stratification of 1981–2011 maize and soybean yields by irrigation regime and agroclimatic zone. Darker colors indicate grid cells with higher yields. Additional crops in Appendix (Fig. A.2). (For interpretation of the references to color in this figure legend, the reader is referred to the Web version of this article.)

coefficients of eq. (2) jointly stratified by agroclimatic zone and irrigation regime. We therefore stratify the parameters along each of these dimensions separately. Additionally, while eq. (2) incorporates both grid-cell and country fixed effects, the latter are not identified when country-level time trends are included. Our final empirical specification therefore includes grid-cell fixed effects and country-level time trends. We assume that representative producers within the same agroclimatic zones and irrigation regime have a similar decision making process, and employ multiway clustered standard errors (Cameron et al., 2011), clustering by country and year[6]

[6] Results are similar when using Conley standard errors (Conley, 1999).

Table 1
Yield responses in US—Rainfed Maize.

	Long differences (15y)				Panel				ECM			
	(1)	(2)	(3)	(4)	(5)	(6)	(7)	(8)	(9)	(10)	(11)	(12)
GDD < 29 °C	−0.0001	−0.0001			−0.0002*	−0.0002*			−0.0001*	−0.00004		
	(0.0002)	(0.0002)			(0.00003)	(0.00003)			(0.00003)	(0.00003)		
GDD > 29 °C	−0.001*	−0.001*			−0.002*	−0.002*			−0.002*	−0.002*		
	(0.0004)	(0.0004)			(0.0002)	(0.0002)			(0.0003)	(0.0003)		
Total P	0.0002*	0.0002*			0.0002*	0.0002*			0.0002*	0.0002*		
	(0.0001)	(0.0001)			(0.00005)	(0.00005)			(0.0001)	(0.0001)		
Total P Squared	−0.00000*	−0.00000*			−0.00000*	−0.00000*			−0.00000*	−0.00000*		
	(0.000)	(0.000)			(0.000)	(0.000)			(0.000)	(0.000)		
$\overline{T} <$ 15°C			0.002	0.002			−0.001+	−0.001			−0.003*	−0.003*
			(0.003)	(0.003)			(0.001)	(0.001)			(0.001)	(0.001)
22.5 °C$\leq \overline{T} <$ 25°C			0.003	0.003			−0.002*	−0.002*			−0.003*	−0.002*
			(0.003)	(0.003)			(0.0004)	(0.0004)			(0.001)	(0.001)
25 °C$\leq \overline{T} <$ 27.5°C			0.0003	0.0003			−0.003*	−0.003*			−0.004*	−0.003*
			(0.002)	(0.002)			(0.001)	(0.0005)			(0.001)	(0.001)
27.5 °C$\leq \overline{T} <$ 30°C			−0.003	−0.003			−0.004*	−0.004*			−0.006*	−0.004*
			(0.002)	(0.002)			(0.001)	(0.001)			(0.001)	(0.001)
$\overline{T} \geq$ 30°C			−0.001	−0.001			−0.010*	−0.009*			−0.010*	−0.009*
			(0.002)	(0.002)			(0.001)	(0.001)			(0.001)	(0.001)
$P <$ 5 mm			−0.001	−0.001			−0.002*	−0.002*			−0.002*	−0.002*
			(0.001)	(0.001)			(0.001)	(0.001)			(0.001)	(0.001)
LR: GDD < 29 °C									0.0001+	0.0002*		
									(0.0001)	(0.0001)		
LR: GDD > 29 °C									−0.001	−0.001		
									(0.001)	(0.001)		
LR: Total P									0.0003*	0.0003*		
									(0.0001)	(0.0001)		
LR: Total P Squared									−0.00000*	−0.00000*		
									(0.000)	(0.000)		
LR: $\overline{T} <$ 15°C											−0.009*	−0.009*
											(0.002)	(0.002)
LR: 22.5 °C$\leq \overline{T} <$ 25°C											−0.004*	−0.004*
											(0.001)	(0.001)
LR: 25 °C$\leq \overline{T} <$ 27.5°C											−0.005*	−0.003*
											(0.002)	(0.002)
LR: 27.5 °C$\leq \overline{T} <$ 30°C											−0.009*	−0.006*
											(0.002)	(0.002)
LR: $\overline{T} \geq$ 30°C											−0.007*	−0.006*
											(0.002)	(0.002)
LR: $P <$ 5 mm											−0.004*	−0.004*
											(0.001)	(0.001)
Error correction coef.									−0.569*	−0.560*	−0.537*	−0.551*
									(0.035)	(0.042)	(0.043)	(0.045)
T LR/SR ratio						0.4[a]		0.1[b]		0.35[c]		0.59[d]
P LR/SR ratio						1.08[e]		0.77[f]		1.35[g]		2.24[h]
N	342	342	342	342	10,490	10,490	10,490	10,490	10,148	10,148	10,148	10,148
Adjusted R^2	0.609	0.611	0.596	0.597	0.827	0.837	0.827	0.834	0.385	0.425	0.381	0.416

Notes: Significance levels $+ p < 0.1$, $^*p < 0.05$. LR indicates long-run effect, the negative of the estimated parameter divided by the error correction coefficient in specifications (9)–(12).

[a] Ratio of GDD29 semi-elasticities in long difference (2) and panel (6) specifications.
[b] Ratio of $\overline{T} \geq 30$°C semi-elasticities in long difference (4) and panel (8) specifications.
[c] Ratio of short- and long-run GDD29 semi-elasticities in ECM specification (10).
[d] Ratio of short- and long-run $\overline{T} \geq 30$°C semi-elasticities in ECM specification (12).
[e] Ratio of precipitation semi-elasticities in long difference (2) and panel (6) specifications.
[f] Ratio of $P < 5$ mm semi-elasticities in long difference (4) and panel (8) specifications.
[g] Ratio of short- and long-run precipitation semi-elasticities in ECM specification (10).
[h] Ratio of short- and long-run $P < 5$ mm semi-elasticities in ECM specification (12).

4. Empirical results

4.1. *Weather sensitivity of US rainfed yields: replicating and extending Burke and Emerick (2016)*

We begin by using our gridded data on yields and weather to replicate Burke and Emerick (2016)'s analysis for rainfed maize and

Table 2
Yield responses in US—Rainfed Soybeans.

	Long differences (15y)				Panel				ECM			
	(1)	(2)	(3)	(4)	(5)	(6)	(7)	(8)	(9)	(10)	(11)	(12)
GDD < 29 °C	0.0001	0.0001			−0.0001*	−0.0001+			−0.0002*	−0.0001*		
	(0.0003)	(0.0003)			(0.00004)	(0.00003)			(0.00003)	(0.00002)		
GDD > 29 °C	−0.002*	−0.002*			−0.004*	−0.004*			−0.004*	−0.004*		
	(0.001)	(0.001)			(0.001)	(0.001)			(0.001)	(0.001)		
Total *P*	−0.00002	−0.00002			0.0001*	0.0001*			0.0002*	0.0002*		
	(0.0001)	(0.0001)			(0.00003)	(0.00003)			(0.00004)	(0.00004)		
Total *P* Squared	−0.000	−0.000			−0.00000*	−0.00000*			−0.00000*	−0.00000*		
	(0.000)	(0.000)			(0.000)	(0.000)			(0.000)	(0.000)		
$\overline{T}$ < 15°C			0.0002	0.001			−0.002*	−0.001*			−0.003*	−0.003*
			(0.003)	(0.003)			(0.0003)	(0.0003)			(0.0005)	(0.0005)
22.5 °C≤ $\overline{T}$ < 25°C			0.002	0.002			−0.001*	−0.001+			−0.002*	−0.002*
			(0.003)	(0.003)			(0.001)	(0.001)			(0.001)	(0.001)
25 °C≤ $\overline{T}$ < 27.5°C			0.0001	0.0002			−0.002*	−0.002*			−0.004*	−0.003*
			(0.003)	(0.003)			(0.001)	(0.0005)			(0.001)	(0.0005)
27.5 °C≤ $\overline{T}$ < 30°C			0.001	0.001			−0.002*	−0.001*			−0.005*	−0.004*
			(0.004)	(0.004)			(0.001)	(0.001)			(0.001)	(0.001)
$\overline{T}$ ≥ 30°C			−0.007	−0.006			−0.012*	−0.012*			−0.014*	−0.014*
			(0.005)	(0.005)			(0.001)	(0.001)			(0.001)	(0.001)
Precip. < 5 mm			0.001	0.001			−0.001	−0.001			−0.0002	−0.0004
			(0.001)	(0.001)			(0.0004)	(0.0004)			(0.0005)	(0.0004)
LR: GDD < 29 °C									−0.0003*	−0.0002*		
									(0.0001)	(0.0001)		
LR: GDD > 29 °C									−0.005*	−0.005*		
									(0.001)	(0.001)		
LR: Total *P*									0.0003*	0.0003*		
									(0.0001)	(0.0001)		
LR: Total *P* Squared									−0.00000*	−0.00000*		
									(0.000)	(0.000)		
LR: $\overline{T}$ < 15°C											−0.007*	−0.007*
											(0.002)	(0.002)
LR: 22.5 °C≤ $\overline{T}$ < 25°C											−0.005*	−0.005*
											(0.002)	(0.002)
LR: 25 °C≤ $\overline{T}$ < 27.5°C											−0.009*	−0.009*
											(0.002)	(0.002)
LR: 27.5 °C≤ $\overline{T}$ < 30°C											−0.013*	−0.012*
											(0.002)	(0.002)
LR: $\overline{T}$ ≥ 30°C											−0.023*	−0.022*
											(0.003)	(0.003)
LR: *P* < 5 mm											−0.002	−0.003*
											(0.001)	(0.001)
Error correction coef.									−0.456*	−0.429*	−0.437*	−0.428*
									(0.029)	(0.039)	(0.035)	(0.043)
T LR/SR ratio						0.62[a]		0.53[b]		1.37[c]		1.64[d]
P LR/SR ratio						−0.17[e]		−2.2[f]		2.15[g]		6.01[h]
N	294	294	294	294	9102	9102	9102	9102	8808	8808	8808	8808
Adjusted R^2	0.408	0.411	0.410	0.412	0.837	0.850	0.832	0.843	0.407	0.426	0.392	0.403

Notes: Significance levels + $p < 0.1$, *$p < 0.05$. LR indicates long-run effect, the negative of the estimated parameter divided by the error correction coefficient in specifications (9)–(12).

[a] Ratio of GDD29 semi-elasticities in long difference (2) and panel (6) specifications.
[b] Ratio of $\overline{T} \geq 30$°C semi-elasticities in long difference (4) and panel (8) specifications.
[c] Ratio of short- and long-run GDD29 semi-elasticities in ECM specification (10).
[d] Ratio of short- and long-run $\overline{T} \geq 30$°C semi-elasticities in ECM specification (12).
[e] Ratio of precipitation semi-elasticities in long difference (2) and panel (6) specifications.
[f] Ratio of $P < 5$ mm semi-elasticities in long difference (4) and panel (8) specifications.
[g] Ratio of short- and long-run precipitation semi-elasticities in ECM specification (10).
[h] Ratio of short- and long-run $P < 5$ mm semi-elasticities in ECM specification (12).

soybeans in the US. Tables 1 and 2 show long-difference, static fixed-effects and ECM estimates of the yield effects of weather exposures specified in two ways. The first, following Burke and Emerick, is growing degree days (GDDs) stratified by days with average temperature ($\overline{T}$) above and below 29 °C, and total growing season precipitation and its square. The second is the annual count of days over the growing season that fall into six temperature (°C) and precipitation (mm/day) intervals (bins).

In Table 1 (maize), coefficients on GDDs > 29 °C (hereafter GDD29) in the long difference and the panel specifications (columns

1–2 and 5–6, respectively) are negative and significant. The ratio of the former to the latter is 0.5, indicating a 50% reduction in the yield impacts of accumulated extreme heat over the long run. This figure mirrors the ratio of the long- and short-run coefficients in the ECM (columns 9–10), which suggests that farmers' adjustments amount to a 50% attenuation in yield sensitivity to accumulated extreme heat over the long run. Our preferred specification using binned weather exposures (columns 3–4, 7–8 and 11–12) highlights the nonlinearity in crop yields' response to temperature, with semi-elasticities of yield that become increasingly negative with exposure to hotter temperatures, corroborating (Schlenker and Roberts, 2009). Compared to GDD29, the effect of $\overline{T} \geq 30°C$ days is much larger for the ratio of the long difference and the panel coefficients (90% attenuation in yield impact over the long run, columns 3 and 7), but the lack of significance of the former estimates prevents us from drawing firm conclusions. In our preferred ECM estimates (columns 11–12) the ratio of the short- and long-run coefficients indicates that adjustment attenuates yield sensitivity by 30–33%.

Similarly in Table 2 (soybeans), the ratio of the GDD29 long difference and panel coefficients is 0.5, indicating a 50% reduction in the impact of accumulated extreme heat. However, the ratio of the ECM long- and short-run GDD29 coefficients exceeds unity, suggesting that adjustments may have had the opposite effect, making production 25% *more* sensitive to accumulated extreme heat. For our preferred bin specification, estimated semi-elasticities of exposure to $\overline{T} \geq 30°C$ days are positive for the ratio of the long-difference and panel coefficients (impact attenuation of 42% over the long-run), but are negative and larger for the ratio of the ECM coefficients (impact amplification of 64% over the long run -columns 11–12, compared to 25% -columns 9–10 for GDD29).

Re-running our suite of regressions for the same panels of grid cells with covariates constructed from the PRISM climate dataset[7] (Appendix Tables A.6 and A.7) produced noisy estimates that precluded precise estimates of adaptation using Burke and Emerick's method. Looking first at maize, in the long difference specification, effects of GDD29 are insignificant, small in magnitude, and of counterintuitive sign, while in the panel specification, their effect is similar in sign but slightly larger in absolute terms to the corresponding estimates in Table 1. By contrast, in the ECM specification, the short- and long-run impacts of GDD29 (columns 9–10) are both negative and significant, and the latter exceeds the former (column 10), indicating that long-run adjustment increases yield sensitivity to accumulated extreme heat by 33%. The results are similar in our preferred specification, in which exposure to $\overline{T} \geq 30°C$ days has an adverse effect on yields that increases by 9% over the long run (column 12). Soybeans exhibit a similar pattern, with long-difference estimates that are of the expected sign but not significant, panel estimates that are negative and two-thirds as large as those in Table 1, and ECM estimates that show near identical short- and long-run impacts for GDD29 (moderate to no attenuation in yield impacts, columns 9–10 in Table A.7). The panel and ECM estimates of the short-run impact of $\overline{T} \geq 30°C$ days are similar, while the long-run impacts are 50–70% larger (columns 11–12).

Tables A.8 and A.9 summarize the results of extending the foregoing analysis to other rainfed crops in the US.[8] Winter wheat's yield sensitivity follows a pattern similar to maize and soybeans, with short- and long-run ECM estimates that suggest that adjustment moderates impacts from GDD29 by 49% and from $\overline{T} \geq 30°C$ days by 19%. Spring wheat yields' sensitivity to extreme heat is less clear cut, with impacts of GDD29 and $\overline{T} \geq 30°C$ that are counterintuitive in sign, most of which are not significant. Exposure to $27.5 \leq \overline{T} < 30°C$ days exhibits impacts of the expected sign in the long-difference, panel and ECM specifications, but are insignificant save for the ECM long run.

Taken together, these results confirm that the long-run equilibrium to which US producers of rainfed maize, soybeans and winter wheat adjust is one in which exposure to daily temperatures in excess of 29 °C continues to substantially reduce yields. Our novels findings are that farmers' adjustment, despite being rapid (our estimated error-correction coefficients indicate adjustment to equilibrium in 1.8–3.5 years), does not necessarily translate into adaptation as conventionally understood in the climate change policy literature. Crucially, impacts of high temperature extremes over the long run do not decline in magnitude relative to those in the short run—quite the opposite, in many cases they increase. One could hypothesize that this result might be due to farmers pursuing "run-of-the-mill" adaptation that lowers the long-run sensitivity of crop yields to *non*-extreme temperatures. Yet, our ECM bin specification estimates in columns 11–12 find no evidence for such behavior. The ratios of long-run to short-run impacts for daily temperature intervals of $27.5 \leq \overline{T} < 30°C$, $25 \leq \overline{T} < 27.5°C$ and even $22.5 \leq \overline{T} < 25°C$ are all larger in magnitude and significant for maize, soybeans and winter wheat.

A second key finding is adverse long-run impacts of extreme low precipitation, an effect that has long been identified by agronomic simulations, but has received limited attention in the empirical impacts literature (Lobell et al., 2011). The panel and ECM bin specifications show impacts of days with total precipitation $P < 5$ mm that are negative and in the short run one quarter as large as those with $\overline{T} \geq 30°C$ in the case of maize and winter wheat. Compared to the effects of extreme high temperatures, the corresponding long-run ECM impacts are two thirds as large for maize, 14% as large for soybeans, and one-third as large for winter wheat. For spring wheat, the negative impact of $P < 5$ mm days slightly exceeds that for $\overline{T} \geq 30°C$ days in the panel specification (though the latter is not significant) and for $27.5 \leq \overline{T} < 30°C$ in the long-run component of the ECM. Moreover, the long-run sensitivity to $P < 5$ mm days exceeds its short-run counterpart for all crops, and the ratio of the former to the latter is generally larger than that for $\overline{T} \geq 30°C$ days.

The key implication of these results is that farmers' adjustment may increase the vulnerability of crop yields to adverse weather shocks.

[7] Parameter-elevation Regressions on Independent Slopes Model (PRISM), Climate Group, Oregon State University, http://prism.oregonstate.edu, accessed on 10 October 2019.

[8] The sample of cells with rainfed rice was too small to permit estimation.

Table 3
Yield responses in Rest of World—Rainfed Maize.

	Long differences (15y)				Panel				ECM			
	(1)	(2)	(3)	(4)	(5)	(6)	(7)	(8)	(9)	(10)	(11)	(12)
GDD < 29 °C	0.0001	0.0001			−0.0004*	−0.0004*			−0.0004*	−0.0004*		
	(0.0002)	(0.0002)			(0.0001)	(0.0001)			(0.0001)	(0.0001)		
GDD > 29 °C	−0.001	−0.001			−0.001*	−0.001*			−0.001*	−0.001*		
	(0.001)	(0.001)			(0.0004)	(0.0003)			(0.0004)	(0.0003)		
Total *P*	0.00002	0.00002			0.00004*	0.00004*			0.00004*	0.00004*		
	(0.00002)	(0.00002)			(0.00001)	(0.00001)			(0.00001)	(0.00001)		
Total *P* Squared	−0.000	−0.000			−0.000*	−0.000*			−0.000*	−0.000*		
	(0.000)	(0.000)			(0.000)	(0.000)			(0.000)	(0.000)		
$\overline{T}$ < 15°C			−0.0002	−0.0002			0.001	0.001+			0.001	0.001
			(0.001)	(0.001)			(0.001)	(0.001)			(0.001)	(0.001)
22.5 °C≤ $\overline{T}$ < 25°C			0.0002	0.0002			−0.003*	−0.003*			−0.003*	−0.003*
			(0.001)	(0.001)			(0.001)	(0.001)			(0.001)	(0.001)
25 °C≤ $\overline{T}$ < 27.5°C			−0.0002	−0.0002			−0.004*	−0.004*			−0.004*	−0.004*
			(0.001)	(0.001)			(0.001)	(0.001)			(0.001)	(0.001)
27.5 °C≤ $\overline{T}$ < 30°C			−0.00001	−0.00003			−0.005*	−0.005*			−0.005*	−0.005*
			(0.001)	(0.001)			(0.001)	(0.001)			(0.001)	(0.001)
$\overline{T}$ ≥ 30°C			−0.004	−0.004			−0.009*	−0.010*			−0.010*	−0.010*
			(0.002)	(0.002)			(0.002)	(0.002)			(0.002)	(0.002)
P < 5 mm			−0.002*	−0.002*			−0.003*	−0.003*			−0.004*	−0.004*
			(0.001)	(0.001)			(0.001)	(0.001)			(0.001)	(0.001)
LR: GDD < 29 °C									−0.0004*	−0.0004*		
									(0.0001)	(0.0001)		
LR: GDD > 29 °C									−0.0003	−0.001		
									(0.001)	(0.0004)		
LR: Total *P*									0.0001*	0.0001*		
									(0.00001)	(0.00001)		
LR: Total *P* Squared									−0.000*	−0.000*		
									(0.000)	(0.000)		
LR: $\overline{T}$ < 15°C											0.002+	0.002+
											(0.001)	(0.001)
LR: 22.5 °C≤ $\overline{T}$ < 25°C											−0.002*	−0.003*
											(0.001)	(0.001)
LR: 25 °C≤ $\overline{T}$ < 27.5°C											−0.004*	−0.004*
											(0.001)	(0.001)
LR: 27.5 °C≤ $\overline{T}$ < 30°C											−0.005*	−0.005*
											(0.001)	(0.001)
LR: $\overline{T}$ ≥ 30°C											−0.008*	−0.008*
											(0.002)	(0.002)
LR: *P* < 5 mm											−0.004*	−0.004*
											(0.001)	(0.001)
Error correction coef.									−0.853*	−0.861*	−0.849*	−0.856*
									(0.033)	(0.034)	(0.034)	(0.035)
T LR/SR ratio						0.97[a]		0.37[b]		0.47[c]		0.81[d]
P LR/SR ratio						0.56[e]		0.63[f]		1.27[g]		1.23[h]
N	1237	1229	1237	1229	36,368	34,161	36,368	34,161	35,070	32,821	35,070	32,821
Adjusted R^2	0.744	0.741	0.744	0.741	0.915	0.917	0.916	0.918	0.455	0.461	0.462	0.468

Notes: Significance levels + $p < 0.1$, *$p < 0.05$. LR indicates long-run effect, the negative of the estimated parameter divided by the error correction coefficient in specifications (9)–(12).

[a] Ratio of GDD29 semi-elasticities in long difference (2) and panel (6) specifications.
[b] Ratio of $\overline{T} \geq 30$°C semi-elasticities in long difference (4) and panel (8) specifications.
[c] Ratio of short- and long-run GDD29 semi-elasticities in ECM specification (10).
[d] Ratio of short- and long-run $\overline{T} \geq 30$°C semi-elasticities in ECM specification (12).
[e] Ratio of precipitation semi-elasticities in long difference (2) and panel (6) specifications.
[f] Ratio of $P < 5$ mm semi-elasticities in long difference (4) and panel (8) specifications.
[g] Ratio of short- and long-run precipitation semi-elasticities in ECM specification (10).
[h] Ratio of short- and long-run $P < 5$ mm semi-elasticities in ECM specification (12).

4.2. Weather sensitivity of global rainfed crop yields

This section addresses the extent to which our US results are representative of broader patterns of yield sensitivity to weather extremes in the rest of the world. Tables 3 and 4 summarize the results for maize and soybeans, results for other calorie crops are relegated to the Appendix (Tables A.10-A.12). Long-difference estimates are for the most part not significant, but indicate modest negative impacts of GDD29 for every crop except soybeans. Panel and short-run ECM estimates of GDD >29 impact are similarly significant, negative and modest in magnitude for maize, soybeans and rice. Long-run ECM estimates are significant only for soybeans,

Table 4
Yield responses in Rest of World—Rainfed Soybeans.

	Long differences (15y)				Panel				ECM			
	(1)	(2)	(3)	(4)	(5)	(6)	(7)	(8)	(9)	(10)	(11)	(12)
GDD < 29 °C	0.00004	0.00004			−0.0001	−0.0002^{+}			−0.0002	−0.0003^{+}		
	(0.0003)	(0.0003)			(0.0002)	(0.0001)			(0.0002)	(0.0001)		
GDD > 29 °C	0.002	0.002			−0.003*	−0.003*			−0.003*	−0.003*		
	(0.002)	(0.002)			(0.001)	(0.001)			(0.001)	(0.001)		
Total *P*	0.0001	0.0001			0.0001*	0.0001*			0.0001*	0.0001*		
	(0.00005)	(0.00005)			(0.00004)	(0.00004)			(0.00004)	(0.00004)		
Total *P* Squared	−0.000	−0.000			−0.000*	−0.000*			−0.000*	−0.000*		
	(0.000)	(0.000)			(0.000)	(0.000)			(0.000)	(0.000)		
$\overline{T}$ < 15°C			−0.005	−0.005			0.001	0.002			0.002	0.003^{+}
			(0.005)	(0.005)			(0.001)	(0.001)			(0.001)	(0.001)
22.5 °C≤ $\overline{T}$ < 25°C			−0.003	−0.003			−0.001	−0.002*			−0.001	−0.002*
			(0.003)	(0.003)			(0.001)	(0.001)			(0.001)	(0.001)
25 °C≤ $\overline{T}$ < 27.5°C			−0.002	−0.002			−0.002	−0.002^{+}			−0.002	−0.003^{+}
			(0.003)	(0.003)			(0.001)	(0.001)			(0.001)	(0.001)
27.5 °C≤ $\overline{T}$ < 30°C			−0.004	−0.004			−0.003	−0.004*			−0.003	−0.004*
			(0.003)	(0.003)			(0.002)	(0.002)			(0.002)	(0.002)
$\overline{T}$ ≥ 30°C			−0.005	−0.005			−0.010*	−0.012*			−0.009*	−0.011*
			(0.004)	(0.004)			(0.004)	(0.005)			(0.004)	(0.005)
P < 5 mm			−0.005	−0.005			−0.003	−0.003			−0.003	−0.003
			(0.003)	(0.003)			(0.002)	(0.002)			(0.002)	(0.002)
LR: GDD < 29 °C									−0.0002	−0.0002*		
									(0.0001)	(0.0001)		
LR: GDD > 29 °C									−0.001*	−0.001*		
									(0.0005)	(0.0005)		
LR: Total *P*									0.0002*	0.0002*		
									(0.00004)	(0.00004)		
LR: Total *P* Squared									−0.000*	−0.000*		
									(0.000)	(0.000)		
LR: $\overline{T}$ < 15°C											0.002	0.003*
											(0.002)	(0.002)
LR: 22.5 °C≤ $\overline{T}$ < 25°C											−0.002	−0.002*
											(0.001)	(0.001)
LR: 25 °C≤ $\overline{T}$ < 27.5°C											−0.002	−0.002*
											(0.001)	(0.001)
LR: 27.5 °C≤ $\overline{T}$ < 30°C											−0.003*	−0.003*
											(0.001)	(0.001)
LR: $\overline{T}$ ≥ 30°C											−0.007*	−0.008*
											(0.002)	(0.003)
LR: *P* < 5 mm											−0.004^{+}	−0.004^{+}
											(0.002)	(0.002)
Error correction coef.									−0.868*	−0.875*	−0.881*	−0.890*
									(0.026)	(0.027)	(0.024)	(0.024)
T LR/SR ratio						−0.56[a]		0.39[b]		0.52[c]		0.71[d]
P LR/SR ratio						0.55[e]		1.97[f]		1.23[g]		1.52[h]
N	733	733	733	733	21,896	18,872	21,896	18,872	21,163	18,071	21,163	18,071
Adjusted R^2	0.414	0.413	0.427	0.426	0.844	0.836	0.838	0.828	0.479	0.489	0.453	0.459

Notes: Significance levels $+ p < 0.1$, $*p < 0.05$. LR indicates long-run effect, the negative of the estimated parameter divided by the error correction coefficient in specifications (9)–(12).

[a] Ratio of GDD29 semi-elasticities in long difference (2) and panel (6) specifications.
[b] Ratio of $\overline{T} \geq 30$°C semi-elasticities in long difference (4) and panel (8) specifications.
[c] Ratio of short- and long-run GDD29 semi-elasticities in ECM specification (10).
[d] Ratio of short- and long-run $\overline{T} \geq 30$°C semi-elasticities in ECM specification (12).
[e] Ratio of precipitation semi-elasticities in long difference (2) and panel (6) specifications.
[f] Ratio of $P < 5$ mm semi-elasticities in long difference (4) and panel (8) specifications.
[g] Ratio of short- and long-run precipitation semi-elasticities in ECM specification (10).
[h] Ratio of short- and long-run $P < 5$ mm semi-elasticities in ECM specification (12).

which exhibits a 66% reduction in sensitivity to accumulated extreme heat over the long run.

In our preferred bin specification, the yield impacts of days with $\overline{T} \geq 30$°C and $P < 5$ mm are generally negative. Long-difference estimates are rarely significant. Panel and short-run ECM estimates of temperature impacts are significant and modestly sized for maize, soybeans and rice, and precipitation impacts are significant for maize and wheat, with the two specifications exhibiting nearly identical results. The patterns of sign and significance are similar for long-run ECM estimates, with significant negative effects of extreme high temperatures on maize, soybeans and rice, and of extreme low precipitation on all crops—with particularly large impacts on spring wheat. Compared to our US results, long-run temperature impacts were one-half to one-sixth as large for maize, soybeans and

Table 5
Yield response to extreme high temperature and low precipitation exposures, by region and irrigation regime.

	USA	Americas	Europe	Asia	Africa	Zone 1	Zone 2	Zone 3
	Rainfed: $\overline{T} \geq 30$°C							
Maize	−0.006	−0.008	[b]	−0.002	−0.015[d]	−0.008	−0.007	−0.01
Rice	[c]	0.005	[c]	[b]	−0.011[d]	−0.01[d]	0.006	[b]
Soybeans	−0.022[d]	−0.012	[c]	−0.008	[b]	−0.005	−0.035[d]	−0.013
Spring Wheat[a]	−0.015	−0.01[d]	−0.016[d]	0.01	[b]	[b]	[b]	−0.009[d]
Winter Wheat	−0.009	−0.014[d]	[b]	[b]	[b]	0.012	[b]	−0.01[d]
	Rainfed: $P < 5$ mm							
Maize	−0.004[d]	−0.004[d]	−0.003	−0.001[d]	−0.009	−0.003[d]	[b]	−0.008[d]
Rice	[c]	−0.001	[c]	[b]	[b]	[b]	0.002	−0.001
Soybeans	−0.003	−0.003[d]	[b]	[b]	−0.01[d]	[b]	[b]	−0.004[d]
Spring Wheat	−0.016[d]	−0.011[d]	0.002	−0.012	[b]	0.004	−0.015[d]	−0.007
Winter Wheat	−0.003	−0.002	−0.002	−0.003	−0.013	0	−0.005	−0.004
	Irrigated: $\overline{T} \geq 30$°C							
Maize	−0.015[d]	−0.013	[b]	[b]	[b]	−0.01	[b]	−0.006
Rice	0.01	[b]	[b]	[b]	−0.011[d]	−0.003	[b]	[b]
Soybeans	−0.025[d]	[c]	[c]	[b]	[c]	[b]	[c]	−0.018[d]
Spring Wheat[a]	[c]	[c]	[c]	[b]	[c]	0.008	[c]	[b]
Winter Wheat	0.011	[b]	[c]	0.004	[b]	[b]	0.003	[b]
	Irrigated: $P < 5$ mm							
Maize	−0.004	−0.007[d]	−0.002	−0.004[d]	−0.014[d]	−0.002	[b]	−0.01[d]
Rice	[b]	−0.001	0.002	0.001	[b]	−0.002[d]	[b]	0.002
Soybeans	−0.009[d]	[c]	[c]	[b]	c	0.005	[c]	[b]
Spring Wheat	[c]	[c]	[c]	[b]	[c]	[b]	[c]	[b]
Winter Wheat	−0.002[d]	[b]	[c]	−0.004[d]	[b]	[b]	−0.006[d]	−0.003

[a] Coefficient on 27.5 °C ≤ T < 30 °C bin (while all coefficients refer to the $T \geq 30$ °C bin, for spring wheat the more significant 27.5 °C ≤ T < 30 °C bin is shown).
[b] Not significant at the 10% level.
[c] Insufficient observations.
[d] Adaptation ratio > 1.

rice, and long-run precipitation impacts were of similar magnitude for maize and soybeans, and half as large for wheat.

Despite their qualitative similarity to our results for the US, the smaller magnitude of impacts raises questions of potential for aggregation bias. As well, estimated rate of adjustment toward equilibrium is nearly instantaneous, with the error-correction coefficients indicating that farmers adjust fully in a little over a year. But perhaps the biggest substantive difference is that the magnitudes of the long-run and short-run ECM parameter estimates indicate that the effects of $\overline{T} \geq 30$°C days are attenuated by 19%, 29%, 74% for maize, soybeans and winter wheat, respectively, while only the impact on rice is amplified—by a slight 9%. This result indicates that, on average, producer adjustment is associated with increased resilience to the effects of extreme high temperatures outside the US. However, this result does not hold for extreme low precipitation. Similar to in the US, impacts of $P < 5$ mm days are between 5% and 52% larger in the long-run for most crops (spring wheat is the exception).

An important question raised by these results is whether the benefits of vulnerability reduction accrue to rich nations with advanced agricultural systems, or to developing countries. Precisely where in the world these impacts arise, and whether the apparently maladaptive consequences of adjustment are concentrated in a few regions, will be apparent from more fine-grained regional stratification of estimates. It is to this we now turn.

4.3. *Regional crop yield sensitivity in the long-run: the role of irrigation*

In this section we address two questions: which regions are especially vulnerable to the adverse effects of weather extremes on rainfed yields, and to what extent are these impacts moderated by irrigation, which is *the* principal adaptation to extreme heat. With warming temperatures, it is anticipated that farmers will increase both irrigated area under cultivation and crop water application over the course of the growing season. However, adjustment along this adaptation margin will only be effective if there is sufficient water available for irrigation: in particular, declines in growing season precipitation—and more extreme low precipitation days, will likely constrain irrigation that is reliant on surface water, hindering the moderating effect on the yield impacts of heat. To conserve space, we focus on the results of our preferred binned weather specification, estimated via ECM. Detailed results are consigned to an online appendix (rainfed crops are summarized in Tables B.1-B.33 and irrigated crops in Tables B.34-B.65).

Table 5 summarizes the regional breakdown in the long-run responses of calorie crop yields to $\overline{T} \geq 30$°C and $\overline{P} < 5$mm days. Yields exhibit negative long-run responses to high temperature extremes in more than half, and to low precipitation extremes in nearly 70%, of rainfed crop × region combinations. Adverse effects are concentrated in the Americas, including the US, and to a lesser extent,

Table 6
Change in extreme high temperature and low precipitation days, 2080–2099 mean relative to 1986–2005 mean, by region and irrigation regime (RCP 8.5).

	USA			Americas			Europe			Asia			Africa			Zone 1			Zone 2			Zone 3		
	Rainfed: $T \geq 30$ °C																							
Maize	**33**.10	**[0**.45,	**94]**	18.10	[0,	150]	6.90	[0,	56]	12.25	[0,	110]	**34**.80	**[0**,	**120]**	**22**.85	**[0**,	**120]**	**83**.90	**[0**,	**160]**	**15**.30	**[0**,	**94]**
Rice	76.50	[56,	94]	86.25	[0,	160]				9.35	[0,	120]	**37**.75	**[0**,	**140]**	40.30	[0,	160]	72.70	[0,	160]	70.65	[0,	170]
Soybeans	**42**.40	**[1**,	**99]**	**46**.40	**[0**.5,	**140]**	3.40	[0,	57]	**16**.30	**[0**,	**100]**	13.65	[0,	110]	**19**.30	**[0**,	**96]**	**83**.90	**[0**.9,	**140]**	**51**.30	**[0**.3,	**130]**
Spring Wheat	**10**.95	**[0**,	**36]**	0.90	[0,	13]	**6**.40	**[0**,	**32]**	6.60	[0,	42]	0.75	[0,	110]	4.65	[0.05,	29]	5.30	[0,	40]	1.95	[0,	38]
Winter Wheat	**8**.15	**[0**,	**29]**	2.40	[0,	63]	0.60	[0,	16]	3.40	[0,	44]	2.10	[0,	35]	4.70	[0,	25]	15.55	[0,	72]	1.95	[0,	26]
	Rainfed: $P < 5$ mm																							
Maize	0.15	[-6.8,	9.6]	0.70	[-8.4,	21]	**5**.00	**[**-3.4,	**14]**	−0.65	[-11,	7.1]	0.80	[-15,	12]	−0.10	[-10,	14]	2.20	[-16,	26]	0.75	[-7,	9.2]
Rice	2.45	[-1.2,	11]	3.05	[-12,	26]				−3.75	[-18,	8.4]	0.00	[-16,	16]	0.30	[-14,	15]	1.50	[-13,	23]	3.10	[-16,	32]
Soybeans	0.45	[-7.7,	8.3]	0.70	[-9.6,	14]	3.35	[-8.5,	17]	−2.50	[-12,	7.2]	1.25	[-7,	7.9]	−0.65	[-9.3,	7.4]	3.25	[-15,	16]	−0.10	[-11,	11]
Spring Wheat	−0.25	[-3.7,	4.6]	−0.35	[-8.2,	5]	1.45	[-4.3,	8.2]	0.65	[-4.1,	5.1]	−6.30	[-38,	10]	0.75	[-4.2,	7.1]	0.85	[-3.6,	5.9]	0.45	[-9.5,	9.3]
Winter Wheat	−1.80	[-9.1,	9.9]	0.70	[-9,	11]	0.70	[-9,	11]	0.70	[-5.9,	9.8]	1.95	[-0.05,	11]	0.55	[-7.9,	14]	0.90	[-2.7,	6.9]	−1.20	[-9.5,	10]
	Irrigated: $T \geq 30$ °C																							
Maize	**34**.40	**[0**,	**93]**	2.00	[0,	120]	14.85	[0,	79]	33.30	[0.3,	88]	7.75	[0,	110]	58.00	[0.1,	100]	**69**.35	**[30**,	**93]**	**22**.55	**[0**,	**81]**
Rice	83.45	[52,	110]	12.95	[0,	150]	4.30	[0,	64]	14.95	[0,	110]	**45**.75	**[0**,	**150]**	**10**.00	**[0**,	**110]**	51.17	[0,	150]	19.40	[0,	170]
Soybeans	**49**.95	**[8**.4,	**90]**	0.15	[0,	100]	0.00	[0,	37]	54.55	[0.55,	100]	61.45	[22,	100]	43.90	[0.05,	99]	74.82	[7.4,	100]	**55**.10	**[0**.6,	**98]**
Spring Wheat	2.55	[0,	43]	0.00	[0,	130]	1.50	[0,	7.5]	2.80	[0,	37]	59.40	[0.55,	130]				5.10	[0,	45]	2.10	[0,	110]
Winter Wheat	2.25	[0,	37]	0.15	[0,	42]				10.10	[0,	44]	10.40	[0,	79]	0.25	[0,	14]	17.85	[0,	54]	0.30	[0,	24]
	Irrigated: $P < 5$ mm																							
Maize	0.10	[-4.4,	7.2]	0.40	[-4.4,	10]	**4**.40	**[**-0.9,	**14]**	0.00	[-7.3,	4.9]	1.85	[-7.1,	7.2]	−0.40	[-9.2,	11]	1.70	[-7.6,	8.6]	0.20	[-4.3,	6.8]
Rice	1.55	[-5.2,	12]	−0.75	[-15,	19]	4.30	[-6.9,	18]	−2.90	[-14,	5.5]	0.60	[-20,	16]	−2.05	[-13,	9.1]	−0.05	[-13,	17]	−1.55	[-18,	27]
Soybeans	1.35	[-4.5,	8]	2.60	[-9.8,	31]	9.05	[-3.1,	23]	−0.70	[-9.9,	8.4]	2.48	[-2.7,	8.4]	−0.20	[-8.8,	7.1]	2.65	[-6.9,	15]	0.30	[-9.7,	10]
Spring Wheat	−0.55	[-4,	2.4]	−8.45	[-20,	4.8]	−3.20	[-7.7,	2.5]	−0.65	[-5.4,	2.7]	1.10	[-5.9,	10]				−0.30	[-2.8,	2.6]	−1.75	[-9.8,	5.5]
Winter Wheat	0.15	[-8.1,	6.1]	1.55	[-1.8,	11]				0.00	[-5.4,	5.2]	0.55	[-0.1,	5.1]	0.65	[-8,	11]	0.15	[-2.3,	4.4]	−1.40	[-8.4,	7]

Table entries show median of the distribution of the present-day to late-century change in the average number of days in each temperature and precipitation interval across cultivated grid cells in each region and 21 climate models. 5th and 95th percentiles of the distribution are shown in square braces. Bold entries indicate the crop × region × irrigation regime combinations for which extreme high temperature and low precipitation exposures have significant negative long-run impacts coincide with a likelihood of substantial increases in exposure to extreme days.

Africa. Asia, and especially Europe experience comparatively few significant impacts. Compared to irrigated cultivation, significant adverse effects of extremes on rainfed crops tend to be more widespread and larger in magnitude. High temperature exposure exerts the dominant effect, with the fractional reduction in annual yields from an additional $\overline{T} \geq 30^{\circ}$C day, an order of two to three times as large as those from an addition $P < 5$ mm day. Extreme heat exposure exerts large reductions on yields of maize and rice in Africa, soybeans and wheat in US and the Americas, and spring wheat in Europe. Dry days have their largest negative effects on yields of maize and winter wheat worldwide-especially in Africa, soybeans in the US and rest of the Americas, and particularly spring wheat in the US, rest of Americas, and Asia.

The results illustrate the effectiveness of irrigation for adaptation to temperature extremes. Irrigated yields respond negatively in the long run to high temperature extremes in 15% of irrigated crop × region combinations, and exhibit positive long-run responses in the case of US rice and winter wheat in the US and Asia. Notwithstanding this, irrigation may not be a panacea, for two reasons. First, across many regions, crop water application has not completely shielded production from the effects of high temperature exposures. Residual adverse yield impacts persist over the long run for maize in US and the Americas, rice in Africa, and soybeans in the US. Second and more worrisome is the broader extent across crops and regions of adverse impacts of dry days over the long run. Irrigated yields respond negatively in the long run to high temperature extremes in more than 35% of irrigated crop × region combinations: maize worldwide, winter wheat in the US and Asia, and particularly soybeans in the US. Although irrigation attenuates both the magnitude and geographic breadth of negative low-precipitation responses, this result suggests that there may be a tradeoff between adaptation to heat versus to drought, with farmers' reliance on irrigation making cultivation more vulnerable to water availability constraints caused by dry growing season days.

Table 5 also sheds light on the extent to which Burke and Emerick's findings apply more broadly. In 36% (42%) of rainfed crop × region combinations where high temperature (low precipitation) has significant adverse long run impacts, the latter responses are larger in magnitude than their short-run counterparts. For irrigated cultivation, the corresponding prevalence of significant and greater than unitary adaptation ratios is 42% and 55%. Thus, even though we cannot observe the individual margins along which farmers adjust within our grid-cell samples, our results demonstrate that, in aggregate across different crops and regions, one-third to one-half of adjustments to a long-run equilibrium in which yields exhibit increased sensitivity to extremes.

An alternative stratification of our data according to Fig. 1's agroclimatic zones tells a consistent story. Yields are significantly adversely affected by high temperature and low precipitation extremes in 60–70% of rainfed crop × AEZ combinations. High temperatures especially reduce maize and soybean yields worldwide; precipitation strongly reduces maize yields in zones 1 and 3, and spring wheat yields in zones 2 and 3. Irrigation moderates but does not completely eliminate—the geographic scope and magnitude of impacts, reducing negative and significant temperature and precipitation responses to 27% and 40%, respectively, of crop × AEZ combinations. About one third of negative long-run impacts are of larger magnitude than their short-run counterparts, corroborating our finding of adjustment leading to worse impacts of weather extremes over the long run.

Finally, we note that the fixed-effects estimates of the yield impacts of extremes are in broad agreement with the patterns reported here, though of course they do not distinguish between short- and long-run impacts (See Appendix Table A.13 for details.).

4.4. *Vulnerability of yields to climate change*

We now consider the implications of our findings for the impacts of future warming. Table 6 summarizes the crop × region × irrigation regime combinations for which vigorous warming simulated by 21 ESMs is predicted to cause substantially more extreme high temperature and low precipitation growing-season days by the end of the century. Increases in the frequency of hot days are ubiquitous, and across ESMs and grid cells their distributions tend to be strongly positively skewed. Median increases are largest in locations in the US, rest of the Americas, and Africa where maize, soybeans and rice are currently cultivated, in US and Europe where spring wheat is grown, and in the US where winter wheat is grown. Comparing the median increases in hot days in areas of rainfed and irrigated cultivation, the exhibit that tend to be larger for in the US, Asia and Africa (an exception is African maize) but smaller throughout the Americas.

By contrast, trends in dry extremes are much less pronounced, reflecting the greater uncertainty in ESM projections of climate change impacts on precipitation. The support of the distribution of changes in $P < 5$ mm days across ESMs and grid cells includes zero for every crop × region × irrigation regime combination, with medians that are negative for 30% of combinations and small in magnitude (fewer than 10 days), and—as with temperature—longer upper tails. The largest median shifts are concentrated in Europe, particularly areas of current rainfed and irrigated maize, and irrigated rice and soybean cultivation.

The table also highlights crop × region × irrigation regime combinations that appear to be especially vulnerable to climate change, i.e., ones for which increases in hot and dry days coincide with significant long-run yield declines associated with those extremes. Corroborating prior studies, we find that the largest vulnerability is associated with shifting temperature extremes, especially for rainfed cultivation. The main hotspots are the US (maize, soybeans and winter wheat) and Africa (maize and rice), as well as soybeans in Asia and the Americas, and spring wheat in Europe. Vulnerability to low precipitation extremes is confined to European maize. The pattern of impacts suggests that while increasing cultivation in currently irrigated areas might reduce these vulnerabilities, there are still likely to be residual risks to US maize and soybeans, African rice, and—for precipitation—European maize.

The foregoing results shed light on yield vulnerability over the very long run. Nearer-term exposures at mid-century time-frames, summarized in Table A.14, exhibit shifts in extreme days that follow a qualitatively similar patterns but are less than half as large, with a substantial fraction being an order of magnitude smaller. Fig. A.3 illustrates that, by comparison, the smaller average temperature rise projected to occur by the 2050s primarily increases the number of *non*-extreme days ($25 \leq \overline{T} < 30$ for maize, soybeans and rice,

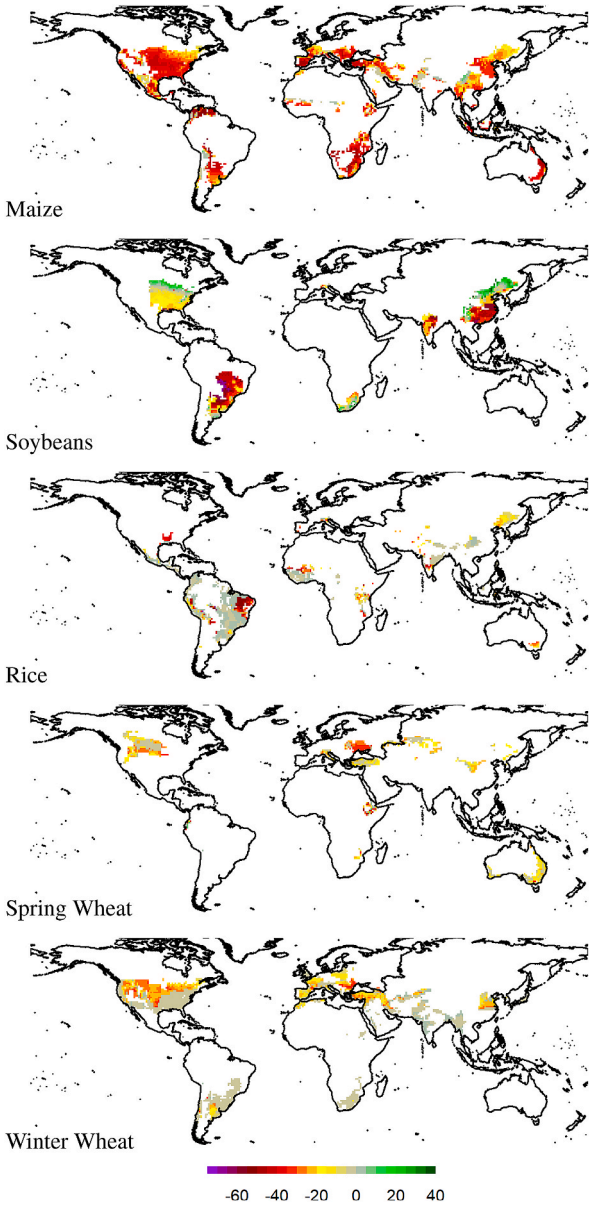

Fig. 2. Climate change impacts on crop yields (%), 2080–2099, median of 21 GCMs, RCP 8.5.

and $22.5 \leq \overline{T} < 27.5$ for wheat). Our preferred specification estimates that negative and significant long-run impacts of days with the latter average temperatures are widespread.[9] Even though the magnitudes of these coefficients are generally smaller than in Table 5, the relatively larger numbers of additional days in the corresponding temperature bins at mid-century suggests that climate change will have discernible impacts on calorie crop yields by 2050. Acceleration of warming toward century's end is accompanied by increases in the number of days in the $27.5 \leq \overline{T} < 30$ interval for all crops, and in the $25 \leq \overline{T} < 27.5$ interval for maize and wheat (Fig. A.3), increasing downward pressure on yields.

5. Projecting the impacts of climate change

We use our fitted econometric model to project the long-run changes in crop yields associated with climatically-driven shifts in

[9] For rainfed crops: maize everywhere except Europe, rice in the Americas, wheat in the US, Americas and Europe, and soybeans in Asia and Africa; for irrigated crops: maize in the US, the Americas and Africa, rice in Asia, soybeans in the US, Americas and Asia, and wheat in the Americas and Asia. See Table 6 and A.14.

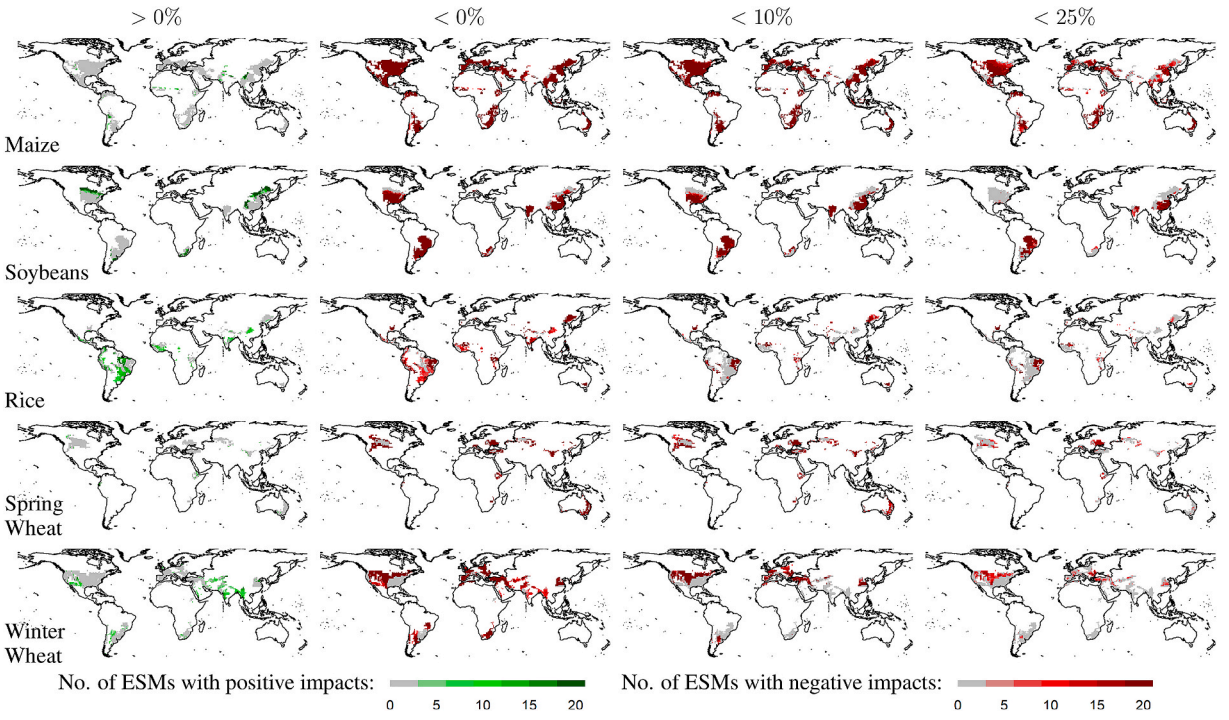

Fig. 3. Agreement among earth system models on yield impacts, 2080–2099: RCP8.5.

meteorological exposure. Let $t = 0$ and $t = t^*$ denote current and future periods, in which the average values of weather exposures are given by $\widetilde{\mathcal{E}}_0^T$ and $\widetilde{\mathcal{E}}_0^P$, and $\widetilde{\mathcal{E}}_{t^*}^T$ and $\widetilde{\mathcal{E}}_{t^*}^P$.

In a changing climate, the weather-sensitive component of log yield with and without adaptation is given by:

$$\Upsilon_{i,0}^{\text{Adaptation}} = \widehat{\boldsymbol{\eta}}_{z(i)}^{T'} \widetilde{\mathcal{E}}_{i,0}^T + \widehat{\boldsymbol{\eta}}_{z(i)}^{P'} \widetilde{\mathcal{E}}_{i,0}^P + \gamma_{j(i)} t^* \tag{8}$$

$$\Upsilon_{i,0}^{\text{No Adaptation}} = \widehat{\boldsymbol{\beta}}_{z(i)}^{T'} \widetilde{\mathcal{E}}_{i,0}^T + \widehat{\boldsymbol{\beta}}_{z(i)}^{P'} \widetilde{\mathcal{E}}_{i,0}^P + \gamma_{j(i)} t^* \tag{9}$$

The time trends $\gamma_{j(i)}t^*$ take into account future exogenous changes in crop productivity. The impacts of climate change on future yields in the presence and absence of adaptation are computed by taking the antilog of the difference between (9) and (8):

$$\phi_{i,t^*}^{\text{Climate, Adaptation}} = \exp\left\{ \widehat{\boldsymbol{\eta}}_{z(i)}^{T'} \left(\widetilde{\mathcal{E}}_{i,t^*}^T - \widetilde{\mathcal{E}}_{i,0}^T \right) + \widehat{\boldsymbol{\eta}}_{z(i)}^{P'} \left(\widetilde{\mathcal{E}}_{i,t^*}^P - \widetilde{\mathcal{E}}_{i,0}^P \right) \right\} \tag{10}$$

$$\phi_{i,t^*}^{\text{Climate, No adaptation}} = \exp\left\{ \widehat{\boldsymbol{\beta}}_{z(i)}^{T'} \left(\widetilde{\mathcal{E}}_{i,t^*}^T - \widetilde{\mathcal{E}}_{i,0}^T \right) + \widehat{\boldsymbol{\beta}}_{z(i)}^{P'} \left(\widetilde{\mathcal{E}}_{i,t^*}^P - \widetilde{\mathcal{E}}_{i,0}^P \right) \right\} \tag{11}$$

Fig. A.3 illustrates the changes in the distribution of average daily temperature over the growing season to which these baseline quantities of crop yields are likely to be exposed, under a high warming (RCP 8.5) scenario. The box plots show the median of our ensemble of ESM projections $\widetilde{\mathcal{E}}_{i,t^*}^T - \widetilde{\mathcal{E}}_{i,0}^T$. Over the annual growing season of our empirical dataset, the temperature shift associated with climate warming induces a decline in cool days and an increase in hot days. At the medians of their respective cultivated grid cells, maize, soybeans and rice experience only slight changes in the number of cool (<10 °C) days, fewer warm (15 − 27.5 °C) days and more frequent hot (≥27.5 °C) days. From mid-to late-century the amplitude of declines in the number of warm days and increases in the number hot days becomes more accentuated, with a marked increase in the frequency of extreme high temperature (≥30 °C) days. Spring wheat's exposure pattern is qualitatively similar, but shifted toward lower temperatures and slightly more pronounced in amplitude, with declines in both cool and moderate temperature days, increases in warm days and little change in the frequency of hot days. Winter wheat exhibits a qualitatively different pattern, made up of modest declines in <5° days that are offset by small increases in the frequency of a broad range of temperatures. As before, these patterns are accentuated with the acceleration of warming toward century's end.

Among the different ESMs there is much less consensus regarding patterns of precipitation exposure (Fig. A.4). Consequently, for all crops the changes in the frequency of growing season days in different intervals of precipitation at the multi-model median ($\widetilde{\mathcal{E}}_{i,t^*}^P - \widetilde{\mathcal{E}}_{i,0}^P$)

are uniformly much smaller, and, for the majority of intervals, less than one day. Exceptions are extreme low (<5 mm) precipitation, which increase by approximately one day for winter wheat circa 2090 and maize at both mid- and late-century, and decline by 1–2 days for rice and soybeans. These two crops also see a slight (1-day) increase in late-century exposure to extreme high (≥55 mm) precipitation.

Given the range of climatic conditions in the grid cells where each crop is grown, there is considerable variation in the aforementioned patterns of climate change exposure[10]. Even so, by mid-century more than three-quarters of the grid cells where each crop is grown experience increases in ≥30 °C days, and a similar fraction of grid cells where spring wheat are grown experience increases in days with <5 mm of precipitation. Given our yield responses in Table 5 and A.13, these shifts raise the possibility that farmers will sustain losses even in the presence of adaptation, and indeed this is exactly what we see.

We estimate the yield impacts of the changes in temperature and precipitation in a high warming scenario (RCP 8.5), at the grid-cell level in the short and the long run, using eqs. (11) and (10). The results of these calculations are summarized graphically in the Appendix (Figs. A.5 and A.6). The crucial implication is that the historical patterns of intra-zonal adjustment inferred by our empirical model suggest that adaptation is unlikely to be a panacea. Not only do our long-run model parameters suggest that changes in yields in response to future climate change will be negative for greater than 75% of grid cell × ESM realizations, but in a few cases in the long run they are worse than in the short run. This phenomenon is of particular concern for irrigated rice, soybeans in zone 1, and winter wheat in zones 1 and 2.[11] The magnitude of impacts is substantial, with interquartile range yield reductions circa 2050 from 3% to 12%, and from 11% to 25% circa 2090.

Impacts are heterogeneous among agroclimatic zones, with some experiencing much larger yield declines than others and no consistent pattern of zonal impacts across crops. With the exception of rice cultivation, irrigation generally moderates the adverse effects of temperature and precipitation change, and for spring wheat may even result in yield improvements (though this effect is more pronounced in the short run). We speculate that residual negative impacts in grid cells that we identify as irrigated may reflect underlying unmeasured irrigation intensity and efficacy, which in turn is a function of water resource scarcity—which we note will also affected by climate change. Regarding the heterogeneity in impacts, the interqartile ranges of yield shocks do not differ dramatically across ESMs. Consequently, the boxplots largely capture the effect of spatial variation in future meteorology.

The manner in which impacts at the median of our ensemble projections (RCP 8.5) plays out over space is elaborated in Fig. 2.[12] Yields decline for most crops in most grid cells, with the largest reductions concentrated in areas that overlap the major calorie sheds. Consistent with Fig. A.5, circa 2050 median yields decline for the majority of cells in the 3%–12% range, interspersed with isolated regions of more severe losses (16–30%). Circa 2090 the latter expand in extent and increase in intensity to 32–57%, particularly for maize, soybeans and wheat.

Looking more holistically at the distribution of impacts across crops in our projection ensemble, we investigate whether our results are due to different ESMs generating similar geographic patterns of impacts on yields (Fig. 3).[13] Strong agreement on gains in crop yields is found for rice across different zones (Brazil, East Africa, Western India), and to a lower extent for wheat (Brazil, India, USA, China, Europe). Models also tend to agree on moderate (0–10%) reductions of yields of maize, soybeans, winnter wheat—less so for spring wheat —across all major cultivating regions. Circa 2050, very large yield losses (>25%) are found across most models in a few grid cells in the United States, Brazil, South Europe, South Africa, South East China, and Australia especially for maize and soybeans. Toward the end of the century, the scope of areas experiencing such severe negative impacts increases substantially and emerge also for wheat especially in United States and North Europe.

6. Discussion and conclusion

We have used gridded crop yield and weather data to empirically model the temperature and precipitation responses of four crops responsible for 75% of global calorie intake. Using a dynamic econometric framework, we distinguish yields' responses in the short run, which we attribute to weather fluctuations—to which we assume farmers are largely unable to adjust, from those in the long run, which we attribute to climate—that manifests itself over long time frames on which we assume that substantial adaptation is possible. In our theoretical set-up, optimizing farmers are assumed to produce the same crop over a fixed amount of available land within each grid cell. In this context, examples of short-run adaptation include changes in the quantity of fertilizers and irrigation, if available. Long-run adaptation could include changes in crop varieties, different planting and harvesting dates, changes in the degree of mechanization as well as different types of nutrients and fertilizers.

Our econometric estimates corroborate Burke and Emerick's (2016) finding of limited historical adaptation in yield responses to weather shocks. Moreover, exploiting the high spatial resolution of the global crop yield dataset, we are able to further extend their results - limited to the United States - to the globe, showing that the inability of historical adaptation to mitigate climate-driven shocks varies significantly across crops, irrigation regime, as well as geographic zones.

[10] The distribution of temperature and precipitation bins in the historical and future periods assembled over the crop-specific regions and growing seasons are shown in appendix Figs. A.11 - A.14.

[11] It is important to keep in mind that our projections are static with respect to the irrigation regime and the agroclimatic zones, which are likely to change in the future.

[12] Results for mid- and end-of-century, and for the RCP 4.5 moderate warming scenario, are summarized in Figs. A.7 and A.8. Both figures' spatial patterns are broadly similar, but smaller in magnitude.

[13] Results for mid- and end-of-century, and for the RCP 4.5 moderate warming scenario, are summarized in Figs. A.9 and A.10.

Projecting climatically-driven changes in crop yields, by combining our estimated responses over the period 1981–2011 with temperature and precipitation fields from an ensemble of climate model simulations, we find substantial agreement among ESMs on crop yield declines of <10% by mid-century and <25% by century's end especially for soybeans, maize, and winter wheat.

Our key finding is that the brunt of yield losses falls on major crop producing and exporting countries. This raises the key question of what additional margins of adjustment beyond those pursued historically (whose net ameliorative effect we have shown to be small) might affect our results. There are many ways in which supply-side adaptation might take place, all of which require additional, deliberate investment. At the intensive margin there is development and diffusion of heat-resistant cultivars, increases in the quantity and/or quality of inputs, or improving management practices for more effective input utilization, and shifting planting and harvesting dates to reduce exposures to high temperatures during particularly vulnerable crop growth phases (e.g., anthesis), or increase the number of annual planting/harvesting cycles. At the extensive margin, farmers in a particular location can switch to crops that are more suitable to changing climatic conditions, or, over broad geographic domains there can be shifts in the locations where crops are grown, non-agricultural land may be brought into cultivation to increase output, or additional land may be irrigated (Sloat et al., 2020), with concomitant increases in surface water diversion or groundwater mining.

Supply-side adjustments, residual supply losses, and increasing world prices of crops and food commodities are likely to be an imperfect form of adjustment. This possibility raises further questions with regards to the potential contribution of demand-side adaptations, such as changes in dietary composition and shifting patterns of international trade. Warming's heterogeneous influences on different crops across locations should not obscure the fact that its fundamental impact is to substantially reduce the supply of crops from all major sources. Improving our understanding of the efficacy of adaptation strategies that might forestalling, or merely lower the cost of coping with, this adverse outcome requires a sustained program of future research.

Our study is not without caveats associated primarily with the high-resolution global gridded crop yield dataset derived using statistical downscaling approaches (see Appendix A for details on how the gridded crop yields are assembled in the Iizumi dataset). As noted by a recent study Yu et al. (2020), more readily available data pertaining to statistics at coarser administrative units, or aggregated data at national scales, do not reveal diversity and spatial patterns, thus making them less informative for subsequent spatially explicit agricultural and environmental analyses. Moreover, downscaling of yield and area harvested statistics onto grids has increasingly provided a basis for recent economic modeling and analysis (see Hertel et al. (2019) for review). For instance, global gridded agricultural datasets have expanded the inclusion of agronomic variables, as examplefied by the recent gridded 'pesticide use' dataset (Maggi et al., 2019) made available by NASA Socioeconomic Data and Applications Center (SEDAC), and another on 'harvested and yield by farming system type' (Yu et al., 2020) provided by the International Food Policy Research Institute (IFPRI).

While the downscaled country-level agricultural production datasets do facilitate a detailed spatiotemporal analysis, their usage under a panel data setting could lead to potential artificial precision in the estimates. For instance, given that the primary input source of data is the country-level data (Fig. A.1), observations within a country could be mechanically correlated.[14] Nevertheless, we believe that this limitation is a trade-off, as the advantage of employing downscaled data outweighs the potential marginal bias in our otherwise precise estimates, as shown by the precision of our estimated coefficients (Readers are guided to Appendix A and B for a full set of regression results). A systematic comparison or meta-analysis of agricultural impacts assessment employing different data sources of climate and agricultural production is left for future research.

Declaration of competing interest

The authors declare there are no conflict of interests.

Acknowledgement

The authors are grateful to T. Iizumi for providing data and clarifications on gridded crop yield and harvested area used in the study; the editor, three anonymous referees, Carlo Fezzi, Luca Fanelli and the participants of the WCERE 2018 - 6th World Congress of Environmental and Resource Economists for constructive feedback on earlier versions of the manuscript; and David Hendry for clarifications on the Error Correction Model. The authors also acknowledge the publicly available climate data sources (NASA-NOAA GLDAS, CMIP5-NASA NEX GDDP) and R packages used in this study. Any remaining errors are those of the authors.

Appendix A. Supplementary data

Supplementary data to this article can be found online at https://doi.org/10.1016/j.jeem.2021.102462.

Data and code

The crop yield, harvested area and growing season calendar data are available from the reference discussion papers cited in this study. Climate data from GLDAS and NASA-NEX GDDP (CMIP5 GCMs) are available from their corresponding data portals. The processed data used in this study are available from the authors upon request.

[14] The amount of independent variation within a country then depends on the relative variances of the country-level FAO data and the NPP data from year-to-year. See Secton A.1 in Appendix for a description of the downscaling methodology in the Iizumi dataset.

References

Blanc, E., Reilly, J., 2017. Approaches to assessing climate change impacts on agriculture: an overview of the debate. Rev. Environ. Econ. Pol. 11 (2), 247–257.

Blanc, E., Schlenker, W., 2017. The use of panel models in assessments of climate impacts on agriculture. Rev. Environ. Econ. Pol. 11 (2), 258–279.

Burke, M., Emerick, K., 2016. Adaptation to climate change: evidence from US agriculture. Am. Econ. J. Econ. Pol. 8 (3), 106–140.

Cameron, A.C., Gelbach, J., Miller, D., 2011. Robust inference with multi-way clustering. J. Bus. Econ. Stat. 29, 238–249.

Cassman, K.G., 1999. Ecological intensification of cereal production systems: yield potential. Soil Qual. Precis. Agric., PNAS 96, 5952–5959.

Challinor, A.J., Watson, J., Lobell, D.B., Howden, S.M., Smith, D.R., Chhetri, N., 2014. A meta-analysis of crop yield under climate change and adaptation. Nat. Clim. Change 4 (4), 287–291.

Conley, T.G., 1999. Gmm estimation with cross sectional dependence. J. Econom. 92, 1–45.

Dell, M., Jones, B.F., Olken, B.A., 2014. What do we learn from the Weather?The new climate–economy literature. J. Econ. Lit. 52 (3), 740–798.

Fanelli, L., 2006. Dynamic adjustment cost models with forward-looking behaviour. Econom. J. 9, 23–47.

Fisher, A.C., Hanemann, W.M., Roberts, M.J., Schlenker, W., 2012. The economic impacts of climate change: evidence from agricultural output and random fluctuations in weather: comment. Am. Econ. Rev. 102 (7), 3749–3760.

Food, U.N., Agriculture Organization, 2003. Food Energy—Methods of Analysis and Conversion Factors, FAO Food & Nutrition Paper No. 77. Rome: FAO.

Hallam, Z., Zanoli, R., 1993. Error correction models and agricultural supply response. Eur. Rev. Agric. Econ. 20, 151–166.

Hartigan, J.A., Wong, M.A., 1979. A K-means clustering algorithm. Appl. Stat. 28, 100–108.

Hertel, T.W., West, A.P.T., Börner, J., Villoria, N.B., 2019. A review of global-local-global linkages in economic land-use/cover change models. Environ. Res. Lett. 14, 053003.

Iizumi, T., Ramankutty, N., 2016. Changes in yield variability of major crops for 1981–2010 explained by climate change. Environ. Res. Lett. 11, 034003.

Iizumi, T., Yokozawa, M., Sakurai, G., Travasso, M., Romanenkov, V., Oettli, P., Newby, T., Ishigooka, Y., Furuya, J., 2014. Historical changes in global yields: major cereal and legume crops from 1982 to 2006. Global Ecol. Biogeogr. 23, 346–357.

Lobell, D.B., Schlenker, W., Costa-Roberts, J., 2011. Climate trends and global crop production since 1980. Science 333, 616–620.

Maggi, F., Tang, F.H.M., Cecilia, D. la, McBratney, A., 2019. PEST-CHEMGRIDS, global gridded maps of the top 20 crop-specific pesticide application rates from 2015 to 2025. Nat. Sci. Data 6 (170), 1–20.

Mendelsohn, R., Massetti, E., 2017. The use of cross-sectional analysis to measure climate impacts on agriculture: theory and evidence. Rev. Environ. Econ. Pol. 11 (2), 280–298.

Monfreda, C., Ramankutty, N., Foley, J.A., 2008. Farming the planet: 2. Geographic distribution of crop areas, yields, physiological types, and net primary production in the year 2000. Global Biogeochem. Cycles 22, GB1022.

Moschini, G.C., 2001. Production risk and the estimation of ex-ante cost functions. J. Econom. 100, 357–380.

Nickell, S., 1985. Error correction, partial adjustment and all that: an expository note. Oxf. Bull. Econ. Stat. 47, 119–129.

Pope, R., Just, R.E., 1996. Empirical implementation of ex ante cost functions. J. Econom. 72, 231–249.

Portmann, F.T., Siebert, S., Doll, P., 2010. MIRCA2000—global monthly irrigated and rainfed crop areas around the year 2000: a new high-resolution data set for agricultural and hydrological modeling. Global Biogeochem. Cycles 24, GB1011.

Ramankutty, N., Mehrabi, Z., Waha, K., Jarvis, L., Kremen, C., Herrero, M., Rieseberg H., L., 2018. Trends in global agricultural land use: Implications for environmental health and food security. Ann. Rev. Plant Biol. 69 (1), 789–815.

Rodell, M., Houser, P.R., Jambor, U., Gottschalck, J., Mitchell, K., Meng, C.-J., Toll, D., 2004. The global land data assimilation system (GLDAS). Bull. Am. Meteorol. Soc. 85, 381–394.

Sacks, W.J., Deryng, D., Foley, J.A., Ramankutty, N., 2010. Crop planting dates: an analysis of global patterns. Global Ecol. Biogeogr. 19, 607–620.

Schlenker, W., Roberts, M.J., 2009. Nonlinear temperature effects indicate severe damages to U.S. crop yields under climate change. Proc. Natl. Acad. Sci. Unit. States Am. 106, 15594–15598.

Sloat, L.L., Davis, S.J., Gerber, J.S., Moore, F.C., Ray, D.K., West, P.C., Mueller, N.D., 2020. Climate adaptation by crop migration. Nat. Commun. 11, 1243.

Yu, Q., You, L., Wood-Sichra, U., Ru, Y., Joglekar, A.K.B., Fritz, S., Xiong, W., Lu, M., Wu, W., Yang, P., 2020. A cultivated planet in 2010: 2 the global gridded agricultural production maps [preprint] Earth Syst. Sci. Data Discuss.. https://doi.org/10.5194/essd-2020-11. in review.